DOI 10.52209/2706-977X_2026_1_98 **IRSTI 55.57.43** **UDC 621.927**

Determination and Optimization of Working Parameters of a Sheep House Feeding Device Based on the Discrete Element Method

Fan Zhihao[1], **Wen Baoqin**[1], **Reshetnikova O.S**[2*], **Li Jinbin**[1], **He Xiaowei**[3]
[1]School of Mechanical and Electrical Engineering, Shihezi University, Shihezi, China
[2]Abylkas Saginov Karaganda Technical University, Karaganda, Kazakhstan
[3]College of Mechanical and Electrification Engineering, Tarim University, Alar, China
[*]corresponding author

Abstract. To achieve precise feeding, this study coupled a Discrete Element Method (DEM)-based virtual test platform with the Response Surface Method (RSM) to quantitatively evaluate and optimize the effects of traveling speed (X_1), scraper rotation speed (X_2), and conveyor belt speed (X_3) on unit feeding amount (Y_1) and feeding uniformity (Y_2). A simplified core model of the feeding device was established in EDEM, and the cohesive characteristics of Total Mixed Ration (TMR) were characterized using the Hertz–Mindlin with JKR Cohesion contact model. A three-factor, three-level Box–Behnken experimental design was employed to fit quadratic regression models for Y_1 and Y_2. The results indicated that both models were statistically significant ($P < 0.0001$). The significant influencing factors for Y_1 were ranked as $X_1 > X_2 > X_3$, while those for Y_2 were ranked as $X_2 > X_3 > X_1$. Based on the analysis of interaction effects among parameters and multi-objective desirability optimization (targeting Y_1 = 10–12 kg·m^{-1} and maximizing Y_2), the optimal combination was determined as X_1 = 3.05 km·h^{-1}, X_2 = 84.9 r·min^{-1}, and X_3 = 326.5 r·min^{-1}. After rounding for engineering application, X_1 = 3 km·h^{-1}, X_2 = 85 r·min^{-1}, and X_3 = 330 r·min^{-1} yielded verification results of Y_1 = 11.49 kg·m^{-1} and Y_2 = 91.54%, with prediction deviations below 5%. Within the studied geometric and parameter ranges, the material flow remained continuous and stable, without persistent arching or blockage. Therefore, the analysis primarily focused on uniformity and throughput. This study provides executable operational parameters and a transferable parameter design approach applicable to cohesive feed systems.

Keywords: discrete element method, EDEM, response surface method, feeding uniformity, unit feeding amount, Total Mixed Ration (TMR)

Introduction

In large-scale sheep farming, the structure and control method of the feeding device are directly related to feed distribution uniformity and feeding cost [1]. At present, various mechanical feeding systems are employed in sheep houses, including belt conveyors, chain/scraper conveyors, screw augers, throwing-type distributors, and multi-mechanism composite systems [2]. These devices have been widely applied in practical production. Over the past decade, the Discrete Element Method (DEM) has gradually become one of the mainstream approaches for analyzing the flow and discharge behavior of bulk feed materials [3]. Compared with purely empirical or fully physical experiments, DEM offers advantages such as lower computational cost, the ability to observe force and velocity fields at the particle scale [4], and efficient investigation of multi-factor combinations. It is particularly suitable for materials like Total Mixed Ration (TMR), which exhibit cohesiveness and morphological diversity [5].

To achieve high-quality feeding performance, it is essential to optimize both the structural and operational parameters of the device, including the matching of scraper/chain speed and belt speed, vehicle traveling speed, feed-retaining mechanism parameters, as well as material moisture content and adhesion characteristics. DEM provides a controllable "virtual test platform" for this purpose: by configuring contact models and material parameters, it enables simulation of the coupled processes of feeding, conveying, and discharging under various operating conditions. This allows for quantitative analysis of the relationships between unit feeding amount and spatial uniformity, and facilitates parameter screening at lower risk and cost [6]. Among available models, the Hertz–Mindlin with JKR Cohesion contact model has been proven effective in characterizing the cohesive behavior of moist silage, alfalfa stems, and powder-granule mixtures, making it suitable for simulation of feeding processes in sheep houses.

Previous studies have investigated key influencing factors of feeding systems from various perspectives. For instance, the scraper (or chain plate) speed determines the advancement rhythm of the lower material layer; the belt speed, together with the outlet geometry, jointly affects the instantaneous flow rate and the spatial distribution of deposited feed strips; while the traveling speed influences the temporal window of material discharge per unit length. Some research has also focused on the structure of the feed bin and anti-arching mechanisms to reduce blockage risk and improve system stability. However, most of these studies have adopted single-factor or empirical approaches, or have used dry granular materials as substitutes for cohesive TMR, lacking quantitative coupling and systematic optimization of three factors under adhesive model constraints. Moreover, the matching mechanism among the scraper, belt, and traveling speed, the forms of their interaction terms, and their combined effects on feeding uniformity remain without a reproducible framework for statistical modeling and validation [7].

Therefore, this study aims to develop a DEM-based virtual simulation platform for a sheep feeding device to systematically quantify the effects of X_1, X_2, and X_3 on Y_1 and Y_2. Furthermore, it seeks to obtain an optimal, engineering-applicable combination of operating parameters via statistical modeling and multi-objective optimization, thereby providing methodological and data support for the structural design and operational calibration of cohesive TMR feeding systems.

To achieve these objectives, this study first develops a simplified device model in SolidWorks and imports it into EDEM. The Hertz–Mindlin with JKR Cohesion contact model is selected to characterize the adhesion properties of TMR. Building on this, the research investigates the effects of the three key operating parameters (X_1, X_2, and X_3) on Y_1 and Y_2. To obtain engineering-applicable parameter combinations, this study establishes a quadratic regression model using the Box–Behnken design (BBD) and conducts analysis of variance (ANOVA) and residual diagnostics. Finally, the multi-objective desirability function is employed to solve for the optimal parameters under given constraints, which are then validated using rounded values for practical engineering application.

1. Materials and methods

To investigate the effects of different combinations of traveling speed, scraper speed, and conveyor belt speed on feeding performance, a simplified computational domain of the feeding device was established in EDEM. Only the lower structures related to material discharge were retained, including the lower cavity of the feed hopper, the scraper conveying channel, the rotating feed-retaining roller, and the tail-end belt conveyor unit. The vehicle's traveling motion was represented by a constant speed V, implemented through a moving coordinate system to simulate the relative uniform motion of the discharge outlet with respect to the ground. Gravitational acceleration was set to 9.81 $m \cdot s^{-2}$. All walls and metallic components were modeled as rigid boundaries, and the contact interactions between the device and the material were defined as "steel–material" contacts.

The motion boundaries and operating conditions were configured as follows: the scraper, feed-retaining roller, and belt were driven as rigid bodies with prescribed rotational speeds. The level ranges of the three factors were determined based on the adjustable ranges observed in field conditions and verified through preliminary simulations. Specifically, X_1 (traveling speed), X_2 (scraper rotational speed), and X_3 (belt rotational speed) were set within 3–7 $km \cdot h^{-1}$, 65–85 $r \cdot min^{-1}$, and 200–400 $r \cdot min^{-1}$, respectively. The total simulation duration was 10 s, during which 0–2 s corresponded to the particle generation and natural accumulation stage, while 2–10 s represented the steady operating stage. The uniform simulation time step was set to 5×10^{-6} s, and the steady-state analysis window was defined within 3.5–10 s.

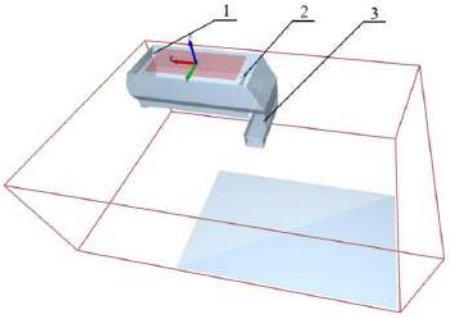

1.Stock bin 2.Material stick 3.Discharge port

Fig.1 - Sketch of EDEM feeding unit

To accurately characterize the adhesion effects among moist organic feed particles and effectively capture the cohesive behavior of the silage and alfalfa particle system, this study employed the Hertz–Mindlin with JKR Cohesion contact model to develop the Discrete Element Method (DEM) simulation framework [8]. To reduce the computational load and enhance simulation efficiency, the actual materials were simplified into equivalent spherical particles with a 5 mm radius, guided by similarity theory[9]. The surface energy parameter of the JKR model was set to 0.27 J/m^2 to reflect the actual adhesion level of the wet TMR [10]. Three representative particle types were constructed based on a mass ratio of 10:5:1 for silage, alfalfa stems, and corn flour, respectively. Their geometries are illustrated in Figure 2. The physical properties of each component are presented in Table 1 [11,12], and the inter-material contact parameters, obtained through literature review and experimental calibration, are listed in Table 2.

Alfalfa stem particles Silage particles Corn meal particles

Fig.2. - Material discrete element model

Table 1. Simulated material characteristics

Material properties	Material type		
	Silage	Corn	Alfalfa
Density(kg/m^3)	195.67	230.23	655.00
Shear modulus(Pa)	7.78×108	2.71×109	1.37×108
Poisson's ratio	0.27	0.23	0.40

Table 2. Contact parameters of materials used in the DEM simulation

Contact pair	Number		
	Static friction coefficient	Rolling friction coefficient	Restitution coefficient
Silage–Silage	0.77	0.14	0.13
Silage–Alfalfa stem	0.52	0.15	0.36
Silage–Corn meal	0.63	0.15	0.12
Silage–Steel	0.58	0.09	0.62
Silage–Ground	0.13	0.01	0.07
Alfalfa stem–Corn particle	0.42	0.19	0.32
Alfalfa stem–Steel	0.41	0.04	0.34
Alfalfa stem–Alfalfa stem	0.37	0.06	0.28
Alfalfa stem–Ground	0.15	0.02	0.10
Corn particle–Corn particle	0.62	0.08	0.11
Corn particle–Steel	0.42	0.05	0.21
Corn particle–Ground	0.10	0.01	0.10

To quantitatively evaluate the effects of the three factors on feeding performance under reproducible conditions and to obtain an engineering-applicable optimal combination, a unified experimental scheme was adopted in this study. First, along the traveling direction, the mass of deposited material on the ground or trough surface was spatially sampled at 1 m intervals . Within the steady-state time window [5, 10, 13] s, the two response indicators, Y_1 and Y_2, were statistically analyzed. Here, Y_1 is defined as the ratio of the total discharged mass during the steady-state stage to the traveling distance, while Y_2 is calculated according to Equations (1) and (2).

$$C_V = \frac{\sqrt{\frac{\sum_{i=1}^{n}(m_i - \overline{m})^2}{n-1}}}{\overline{m}} \quad (1)$$

$$M = 1 - C_V \quad (2)$$

where C_v denotes the coefficient of variation;

m_i represents the mass of the i-th sample (kg);

$\overline{m}_i$ is the average sample mass (kg);

M refers to the feeding uniformity.

Each operating condition was independently repeated three times. To separately investigate the effects of different values of X_1, X_2, and X_3 on Y_1 and Y_2 and to narrow the parameter ranges, single-factor experiments were first conducted by varying one factor while keeping the other two fixed. Subsequently, a three-factor, three-level Box–Behnken Design (BBD) was established to perform combination experiments. The number of center points was set to five or more to estimate pure error, and the experimental sequence was randomized to minimize systematic bias. Each factor was coded as [−1, 0, 1]. Quadratic polynomial models, as expressed in Equation (3), were fitted separately for Y_1 and Y_2. Analysis of variance (ANOVA), lack-of-fit tests, and residual diagnostics were then performed to identify significant factors affecting Y_1 and Y_2. Based on the constraints of experimental parameters, optimization analysis was conducted to determine the optimal combination of parameters. Verification experiments were subsequently performed, and the relative errors were calculated to evaluate the feasibility and robustness of the optimized results.

$$Y = \beta_0 + \sum_{i=1}^{3} \beta_i X_i + \sum_{i=1}^{3} \beta_{ii} X_i^2 + \sum_{i<j} \beta_{ij} X_i X_j \quad (3)$$

2. Results and their discussions

The results of the single-factor experiments for X_1, X_2, and X_3 are shown in the following figures.

Since the time interval between 7–8 s corresponded to a stable feeding stage during the simulations, multiple sampling points within this interval were selected to calculate feeding uniformity.

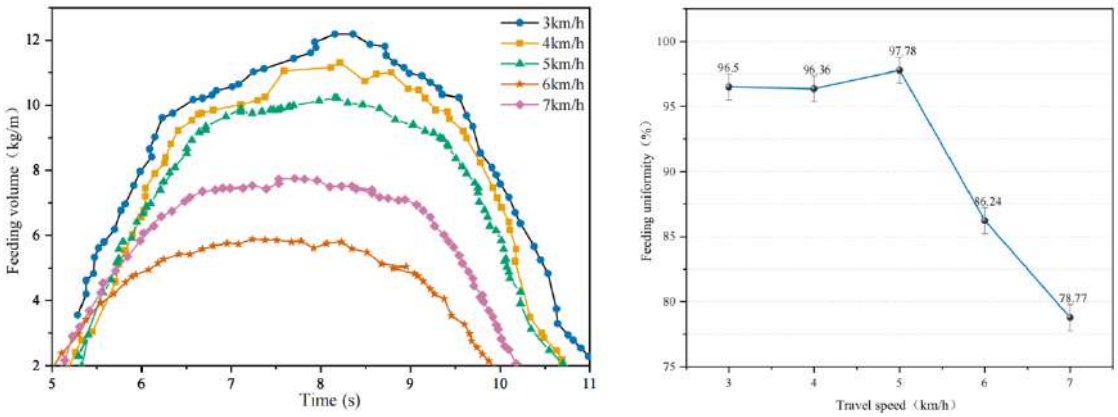

Fig.3. - Effect of X_1 on the feeding volume(Left)and feeding uniformity(Right)when X_2 and X_3 are held constant.

As shown in Fig 3, under constant X_2 and X_3, variation in X_1 affected the length of the feeding strip per unit time. The simulations indicated that as the traveling speed increased from 3–7 km·h^{-1}, the fluctuation of the discharged material intensified and the feeding amount per unit distance decreased. This occurs because particles retained their tangential velocity component from the belt when landing, resulting in greater longitudinal displacement and lateral slip, which in turn reduced feeding uniformity. When the traveling speed exceeded 5 km·h^{-1}, both the unit feeding amount and uniformity fell below acceptable standards. Therefore, the traveling speed range of 3–5 km·h^{-1} was selected for subsequent experiments.

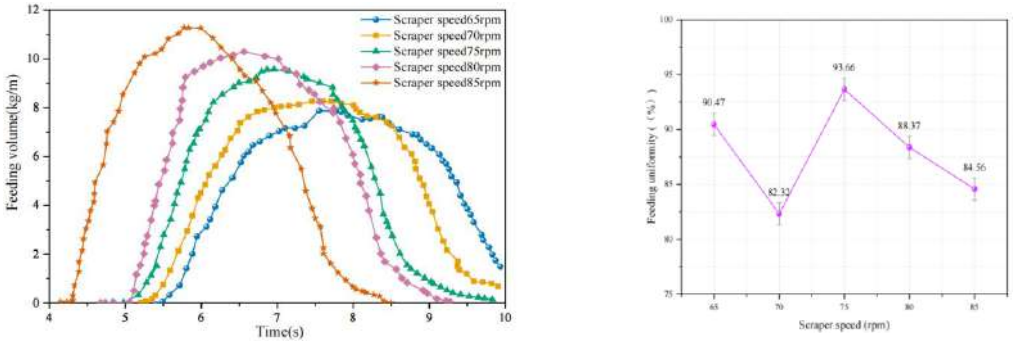

Fig.4. - Effect of X_2 on the feeding volume(Left)and feeding uniformity(Right)when X_1 and X_3 are held constant.

As shown in Fig 4, X_2 (scraper rotational speed) determines the total feeding duration and influences the longitudinal distribution pattern, exhibiting a similar effect to that of X_1. At 85 and 75 r·min^{-1}, significant fluctuations occurred between 6–8 s, whereas the unit feeding amount at 75–80 r·min^{-1} was more consistent, resulting in improved overall uniformity. Considering the operational requirements of sheep housing, scraper speeds between 75–85 r·min^{-1} were found to be suitable; therefore, this range was selected for subsequent tests.

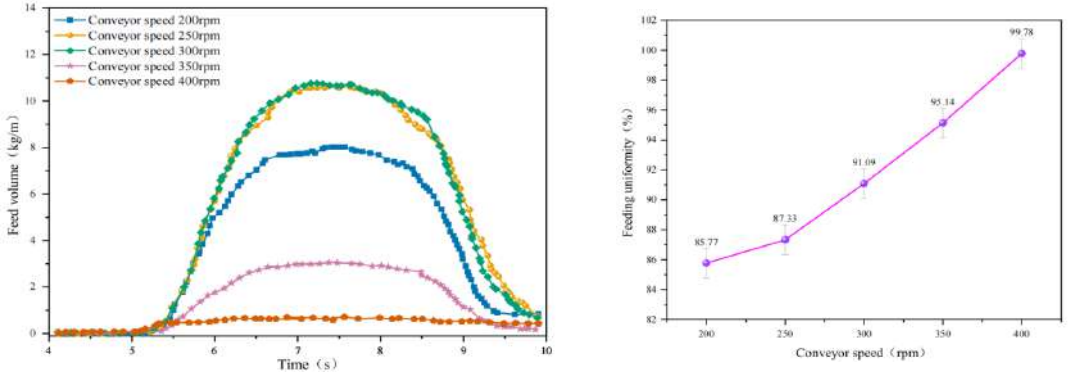

Fig.5. - Material quality chart for different scraper speeds

As shown in Fig 5, X_3 (belt rotational speed) primarily controls the throwing distance of the discharged material. Increasing the belt speed provides particles with higher initial velocity, which enhances landing dispersion and collision, thereby widening the feeding band and breaking up agglomerated particles—ultimately improving feeding uniformity. However, at 400 r·min^{-1}, the throwing distance exceeded the desired range, resulting in material waste, while speeds below 250 r·min^{-1} yielded a unit feeding amount of less than 10 kg·m^{-1}. Consequently, the belt speed range was set between 250–350 r·min^{-1}.

Interaction Effects and Optimization Analysis of Parameters

To further analyze the interactions among multiple factors, a Box–Behnken design (BBD) experiment was conducted as shown in Table 3.

Table 3. Feeding device test program and results

Number	X_1/(km/h)	X_2/(rpm)	X_3/（rpm)	Y_1/(kg/m)	Y_2/(%)
1	-1	-1	0	9.92	76.1
2	1	0	1	7.36	86.4
3	1	1	0	7.58	86.2
4	-1	1	0	12.79	93.7
5	0	1	-1	4.86	81.5
6	1	0	-1	3.42	89.9
7	0	1	1	7.09	80.1
8	0	-1	1	3.47	62.4
9	0	0	0	9.05	85.8
10	1	-1	0	5.82	79.8
11	0	0	0	9.46	86.5
12	-1	0	-1	12.20	93.4
13	0	-1	-1	4.10	69.1
14	0	0	0	9.31	85.4
15	0	0	0	9.46	86.9
16	-1	0	1	9.70	88
17	0	0	0	9.27	86.8

To analyze the influence of experimental factors on the unit feeding amount Y_1, a quadratic regression model of Y_1 with respect to X_1, X_2 and X_3 was established using Design-Expert software. The results showed that the model exhibited a high goodness of fit (R^2=0.98) and was statistically significant (P<0.0001). Regression analysis indicated that X_1, X_2, X_3, X_1X_3, and X_1^2, X_2^2 ,and X_3^2 had highly significant effects on Y^1, while X_2X_3 was significant and X_1X_2 was not significant and therefore removed from the model. The final regression equation is shown in Equation (4). The order of factor influence on Y_1 was X_1>X_2>X_3.

Table 4. Analysis of regression equations for unit feeding quantity

Term	Variance Source	Sum of squares	Degrees of freedom	Mean square	F	P
Y_1	Model	127.93	9	14.21	186.53	< 0.0001
	X_1	52.17	1	52.17	684.53	< 0.0001
	X_2	10.14	1	10.14	133.11	< 0.0001
	X_3	1.15	1	1.15	15.13	0.0060
	X_1X_2	0.3123	1	0.3123	4.10	0.0826
	X_1X_3	10.35	1	10.35	135.76	< 0.0001
	X_2X_3	2.04	1	2.04	26.83	0.0013
	X_1^2	9.53	1	9.53	125.03	< 0.0001
	X_2^2	13.42	1	13.42	176.04	< 0.0001
	X_3^2	29.43	1	29.43	386.20	< 0.0001
	Residual	0.5334	7	0.0762		
	Lack of fit	0.4203	3	0.1401	4.95	0.0782
	Pure error	0.1132	4	0.0283		

$$Y_1 = 9.31 - 2.55X_1 + 1.13X_2 + 0.38X_3 + 1.61X_1X_3 + 0.72X_2X_3 + 1.50X_1^2 - 1.78X_2^2 - 2.64X_3^2 \quad (4)$$

The analysis results of the interaction effects among the experimental parameters are shown in the following figure.

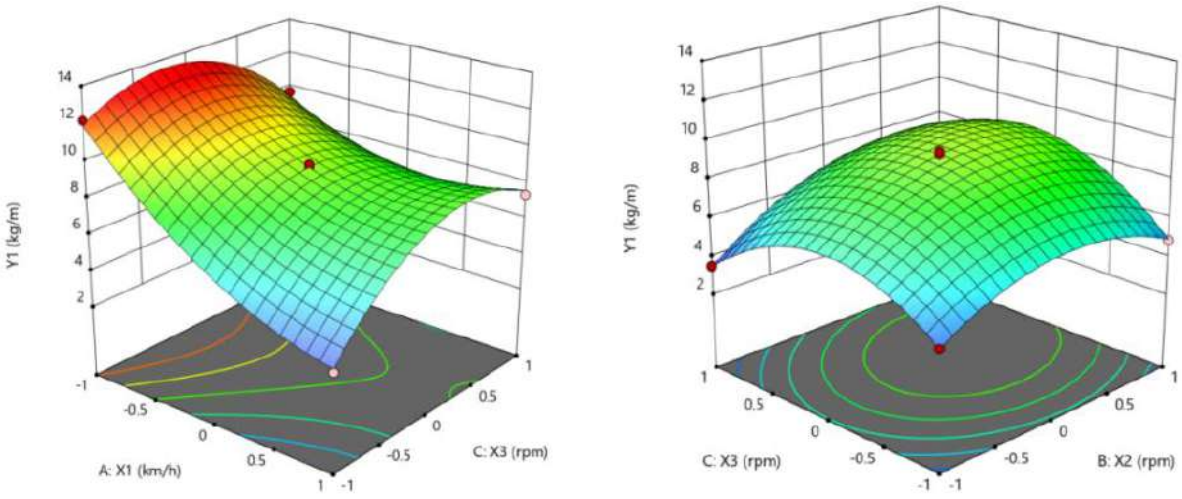

Response surface for the interaction between X_1 and X_3 on Y_1 Response surface for the interaction between X_2 and X_3 on Y_1

Fig.6. - Response surface curves for the interaction of factors on Y1

The two response surfaces show that when X_2 is at its central level (left plot), Y_1 decreases with increasing traveling speed X_1, with a steeper drop at lower levels, and first increases then decreases with belt speed X_3, rising faster at low levels. At the central level, the effect of X_1 on Y_1 is stronger than that of X_3. This occurs because a higher X_1 shortens the feeding duration, reducing the unit feeding amount, while excessive X_3 causes material to be thrown beyond the trough. When X_1 is fixed at its center (right plot), both scraper speed X_2 and belt speed X_3 show an "increase–then–decrease" trend, with X_2 having a more pronounced effect due to excessive shear within the material layer leading to arching and flow interruption. Overall, X_1 has a suppressive effect on Y_1, while X_2 and X_3 exhibit inverted U-shaped influences, with X_2 being dominant.

Similarly, a quadratic regression model of Y_2 with respect to X_1, X_2, and X_3 was constructed using Design-Expert. The model demonstrated excellent goodness of fit (R^2=0.99) and was highly significant (P<0.0001). Regression analysis revealed that X_2, X_3, X_1X_2, and the quadratic terms X_1^2,X_2^2, X_3^2 had extremely significant effects on feeding uniformity (Y^2), while X^1 and X^2X^3 were significant. The non-significant term $X_1X_3$was removed, and the final coded equation model is presented in Equation (5). The order of factor influence on Y_2 was: scraper speed (X_2) > belt speed (X_3) > traveling speed (X_1).

Table 5. Analysis of regression equations for unit feeding quantity

Term	Variance Source	Sum of squares	Degrees of freedom	Mean square	F	P
Y_2	Model	1049.11	9	116.57	122.69	< 0.0001
	X_1	9.90	1	9.90	10.42	0.0145
	X_2	365.85	1	365.85	385.08	< 0.0001
	X_3	36.13	1	36.13	38.02	0.0005
	X_1X_2	31.36	1	31.36	33.01	0.0007
	X_1X_3	0.9025	1	0.9025	0.9499	0.3622
	X_2X_3	7.02	1	7.02	7.39	0.0298
	X_1^2	201.04	1	201.04	211.61	< 0.0001
	X_2^2	359.48	1	359.48	378.38	< 0.0001
	X_3^2	59.69	1	59.69	62.82	< 0.0001
	Residual	6.65	7	0.9501		
	Lack of fit	4.94	3	1.65	3.86	0.1125
	Pure error	1.71	4	0.4270		

$$Y_2 = 86.28 - 1.11X_1 + 6.76X_2 - 2.13X_3 - 2.80X_1X_2 + 1.32X_2X_3 + 6.91X_1^2 - 9.24X_2^2 - 3.77X_3^2 \quad (5)$$

The analysis results of the interactive effects among experimental parameters are presented in the following figure.

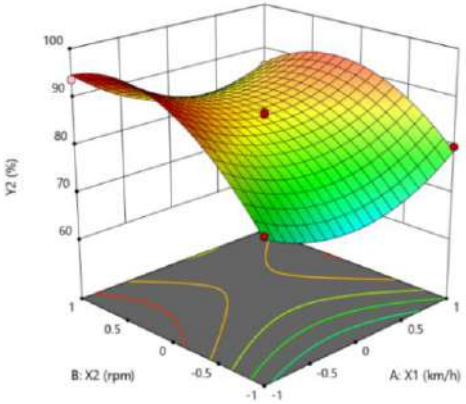

Response surface for the interaction between X_1 and X_2 on Y_2

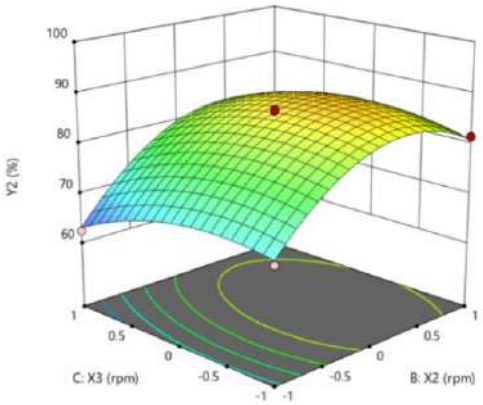

Response surface for the interaction between X_2 and X_3 on Y_2

Fig.7. - Response surface curves for the interaction of factors on Y_2

The two response surfaces indicate that when X_3 is at its central level (left figure), Y_2 (feeding uniformity) exhibits a "decrease–increase" trend with respect to the travel speed X_1, where the decline at lower levels is steeper than the subsequent rise. Its variation with scraper speed X_2 depends on X_1: when X_1 is low, Y_2 increases monotonically with X_2, with a faster rise at lower levels; when X_1 is high, Y_2 first increases and then decreases. When X_1 is fixed at the center (right figure), both X_2 and conveyor speed X_3 show a "rise–fall" effect on Y_2, featuring a faster increase at low levels and a slower decline at high levels. Mechanistically, low levels of X_1, X_2, and X_3 result in insufficient conveying and shearing, causing feed agglomeration and reduced uniformity. As X_2 or X_3 increase, the enhanced linear velocity and shear promote material dispersion through brushing and belt movement, thereby improving uniformity. However, excessive X_1 shortens operation time, overly high X_2 leads to material accumulation and re-agglomeration on the belt, and high X_3 induces similar effects, all of which ultimately reduce feeding uniformity.

Based on practical requirements, the unit feeding rate $Y_1 \in [10,12]$ kg·m^{-1}, while feeding uniformity Y_2 is set as the maximization objective. The decision variables are bounded as follows: travel speed X_1=3 − 5 km· h^{-1}, scraper speed X_2=75-85 rpm, and conveyor speed X3=250 − 350 rpm. On this basis, a constrained optimization model was formulated and Design-Expert's Numerical optimization was employed to obtain the optimal Y_1 and Y_2, as specified below.

$$\begin{cases} 3 \le X_1 \le 5 \\ 75 \le X_2 \le 85 \\ 250 \le X_3 \le 350 \\ 10 \le Y_1 \le 12 \\ maxY_2(X_1,\ X_2,\ X_3,\ X_4) \end{cases} \quad (6)$$

The optimization results indicate that the optimal feeding performance is achieved when the travel speed is 3.05 km h^{-1}, scraper speed 84.9 r min^{-1}, and conveyor speed 326.5 r min^{-1}, corresponding to a unit feeding rate of 11.85 kg m^{-1} and a feeding uniformity of 93.71%. For practical engineering application, the parameters were rounded to 3 km h^{-1}, 85 r min^{-1}, and 330 r min^{-1}, respectively. The control system was then initiated for three validation trials, and the results are summarized in Table 6.

Table 6. Comparison between model optimization value and verification test value

Item	Evaluation Metrics	
	Unit feeding amount (kg·m^{-1})	Feeding uniformity (%)
Model-optimized value	11.85	93.71
Validation (experimental) value	11.49	91.54
Relative error (%)	3.04	2.89

Conclusion

This study successfully combined the Discrete Element Method (DEM) with the Response Surface Method (RSM) to systematically optimize the operating parameters of a sheep house Total Mixed Ration (TMR) feeding device. Through single-factor simulation tests, the effective ranges of the key parameters were first determined: X_1 at 3–5 km/h, X_2 at 75–85 r/min, and X_3 at 250–350 r/min. Based on this, a Box–Behnken design was employed to establish quadratic regression models for Y_1 and Y_2. Analysis of variance (ANOVA) confirmed that both models were highly significant ($P < 0.001$), with goodness-of-fit (R^2) values of 0.98 and 0.99, respectively, indicating high accuracy and strong predictive power. Model analysis quantified the hierarchical order of factor influence: for Y_1, the significance order was $X_1 > X_2 > X_3$, whereas for Y_2, the order was $X_2 > X_3 > X_1$. The study further revealed that X_1 had a significant inhibitory effect on Y_1, while both X_2 and X_3 exhibited an inverted U-shaped influence on Y_2. With the optimization objectives set to maintain Y_1 within 10–12 kg·m^{-1} and maximize Y_2, the optimal parameter combination was determined to be X_1 = 3.05 km·h^{-1}, X_2 = 84.9 r·min^{-1}, and X_3 = 326.5 r·min^{-1}. Under these conditions, the predicted Y_1 and Y_2 were 11.85 kg·m^{-1} and 93.71%, respectively. For practical engineering application, these parameters were rounded to X_1 = 3 km·h^{-1}, X_2 = 85 r·min^{-1}, and X_3 = 330 r·min^{-1}. Subsequent validation experiments yielded a Y_1 of 11.49 kg·m^{-1} and a Y_2 of 91.54%. The relative errors between the experimental and model-predicted values were both below 5%, fully verifying the model's accuracy and the reliability of the optimization. This optimal combination also ensured stable material flow without blockage. This research not only provides executable operational parameters for cohesive feed systems like TMR but also establishes a transferable framework for parameter design and calibration. Future work will focus on investigating the system's adaptability under different operational conditions, such as varying feed formulations or moisture contents, and further enhancing its comprehensive performance.

Acknowledgments

This research was supported by the College of Mechanical and Electrical Engineering at Shihezi University, People's Republic of China. The specific project information is as follows: The agricultural projects of the Xinjiang Production and Construction Corps（NYHXGG,2023AA403; The science and technology program projects of the Xinjiang Production and Construction Corps（2024AB047; The high-level talent research startup projects of Shihezi University（RCZK202310).

References

[1] Xiao J., Sun P. Analysis on the High-end Feeding System and the Application Scenarios on the Lake Sheep Barn Feeding Scale Breeding Technology Research.

[2] Chiu Y.-C., Tsai W.-C., Wu G.-J. W. Developing an Automated Feeding System for Distributing Concentrated Goat Feed // Applied Engineering in Agriculture. American Society of Agricultural and Biological Engineers, 2020. Т. 36, № 2. С. 125–140.

[3] Zhao H. и др. Applications of discrete element method in the research of agricultural machinery: A review // Agriculture. MDPI, 2021. Т. 11, № 5. С. 425.

[4] Zhao J., Zhao S., Luding S. The role of particle shape in computational modelling of granular matter // Nature Reviews Physics. Nature Publishing Group UK London, 2023. Т. 5, № 9. С. 505–525.

[5] Bueno A. V. I. и др. Ensiling total mixed ration for ruminants: a review // Agronomy. MDPI, 2020. Т. 10, № 6. С. 879.

[6] Lu K. и др. Parameter Optimization Method for Centrifugal Feed Disc Discharging Based on Numerical Simulation and Response Surface // Machines. MDPI, 2024. Т. 12, № 11. С. 799.

[7] Ma H. и др. Study on the rigid-discrete coupling effect of scraper conveyor under different chain speed-load conditions // Simulation Modelling Practice and Theory. Elsevier, 2024. Т. 134. С. 102943.

[8] Tao W. U. и др. Calibration of discrete element model parameters for cohesive soil considering the cohesion between particles // Journal of South China Agricultural University. 2023. Т. 38, № 3. С. 93–98.

[9] Chandratilleke G. R., Yu A. B., Bridgwater J. A DEM study of the mixing of particles induced by a flat blade // Chemical Engineering Science. Elsevier, 2012. Т. 79. С. 54–74.

[10 Wu K.-C., You H.-I. Determination of solid material elastic modulus and surface energy based on JKR contact model // Applied surface science. Elsevier, 2007. Т. 253, № 20. С. 8530–8537.

[11] Kaifei W., Baoqin W., Aiken Y., et al. Study on the influence of segmented helical TMR mixer auger structure on mixing performance based on discrete element method // Feed Industry. – 2020. – Vol. 41. – № 19. – pp. 35–41.

[12] Lei W., Yonglin Z., Bin L., et al. Calibration of adhesive parameters for granular feed based on discrete element method and analysis of its crushing process // Feed Industry. – 2023. – Vol. 44. – № 1. – pp. 10–17.

[13] Zharkevich O., Nikonova T., Gierz Ł., Reshetnikova O., Berg A., Warguła Ł., Berg A., Wieczorek B., Łykowski W., Nurzhanova O. Improving the Design of a Multi-Gear Pump Switchgear Using CFD Analysis // Applied Sciences (Switzerland), 2024, 14(13), 5394

Information of the authors

Fan Zhihao, MS, Graduate Student of the School of Mechanical and Electrical Engineering, Shihezi University, and the School of Mechanical Engineering, Karaganda Saginov Technical University.
e-mail:1460220250@qq.com

Wen Baoqin, PhD in Engineering, Doctoral Supervisor, Teaching Expert and Key Faculty Member of Higher Education in Xinjiang Uygur Autonomous Region.
e-mail: wendy-wbq@163.com

Reshetnikova Olga Stasisovna，PhD, acting associate professor**,** Abylkas Saginov Karaganda Technical University.
e-mail: olga.reshetnikova.80@mail.ru

Li Jingbin, PhD in Engineering, Professor (Class II), Doctoral Supervisor, Member of the Standing Committee of the Party Committee and Director of the Publicity Department of Shihezi University, Executive Deputy Director of the Key Laboratory of Modern Agricultural Machinery of XPCC, Deputy Director of the Collaborative Innovation Center for the Modernization of Cotton Production Technology (Co-established by Province and Ministry), Member of the 11th Council of the Chinese Society of Agricultural Engineering, Council Member of the China Mechanical Industry Alliance for Excellent Engineer Education, and Vice Chairman of the Industry-Education Integration Community for Modern Agricultural Machinery and Equipment in China.
e-mail: ljb8095@163.com

He Xiaowei, PhD in Engineering, Associate Professor, Master's Supervisor at Tarim University, and Secretary of the Party Branch of the Department of Agricultural Engineering, College of Mechanical and Electrical Engineering.
e-mail: Hexw_work@163.com